

## 0.25- $\mu\text{m}$ -Emitter InP HBTs with a Passivation Ledge Structure

Norihide Kashio, Kenji Kurishima, Yoshino K. Fukai, Minoru Ida, and Shoji Yamahata

NTT Photonics Laboratories, NTT Corporation  
3-1 Morinosato Wakamiya, Atsugi, Kanagawa 243-0198, Japan  
Phone: +81 46 240 2240, E-mail: kashio@aegl.ntt.co.jp

### 1. Introduction

InP HBTs are promising candidates for ultra-high-speed IC applications to optical fiber communication systems. Recently, there has been a rapid advance in the high-speed performance of InP HBTs with aggressive device scaling [1]. However, a decrease in the device dimension leads to an increase in surface recombination current at the emitter-base periphery, which results in degradation of current gain. Moreover, the surface recombination current may seriously influence device reliability. An effective way to suppress surface recombination current is to form a ledge structure on the extrinsic base region [2]. In this work, we investigated the performance of 0.25- $\mu\text{m}$ -emitter InP HBTs with passivation ledge structures.

### 2. Device structure and fabrication

We used MBE-grown single HBT structures on InP substrates. The base and collector layers are 25-nm-thick p-type InGaAs and 75-nm-thick InGaAs. The base layer was doped to a concentration of  $6 \times 10^{19} \text{ cm}^{-3}$ . The base sheet resistance was estimated to be  $760 \text{ } \Omega/\text{sq.}$  from transmission-line-model measurements. The emitter consists of a degenerately-doped n-type InGaAs layer and a 15-nm-thick undoped InP layer. In this structure, a thin ledge structure can be easily formed by etching the InGaAs cap layer [2].

The device fabrication sequence started with the deposition of W/Au/W films on the emitter cap layer. The upper W film was patterned using i-line lithography and reactive ion etching (RIE). The Au film was etched by inductive coupled plasma (ICP)-RIE with  $\text{Ar}/\text{O}_2$  mixture gas. Here, the upper and bottom W films were used as a mask and etching stopper layer, respectively. After the W films were etched away by RIE, the combination of selective wet etching and ICP-RIE was used to form the emitter mesa. A silicon nitride film was deposited. The silicon nitride film and the InP barrier layer were patterned to cover the extrinsic base region. The barrier layer acts as a ledge layer. Base metals were formed by a lift-off process and electron-beam lithography. The base-collector mesa was formed by wet etching. Each device was isolated by wet etching. For device layout, a base-pad isolation structure was used to eliminate extrinsic base-collector capacitance [3]. Finally, a benzocyclobutene film was spin-coated and cured. Figure 1 shows a SEM image of the fabricated HBT. A 0.25- $\mu\text{m}$ -emitter mesa structure was successfully fabricated. The width of the base metal is 0.25  $\mu\text{m}$  and the emitter-base spacing is 0.15  $\mu\text{m}$ .

### 3. Device characterization

Figure 2 shows the common-emitter collector I-V characteristics. The fabricated HBT provides excellent turn-on characteristics and high collector current density,  $J_c$ , of over  $20 \text{ mA}/\mu\text{m}^2$ . The breakdown voltage,  $BV_{\text{CEO}}$ , is over 2 V. We measured a Gummel plot for the HBT at a collector-base voltage,  $V_{\text{CB}}$ , of 0 V. As shown in Fig. 3, even at a low  $J_c$ , there is no crossover in the Gummel plot. The current gain is 62 at a  $J_c$  of  $10 \text{ mA}/\mu\text{m}^2$ . To investigate the effectiveness of the ledge layer further, we measured Gummel plots of HBTs with various emitter-base spacing. Figure 4 shows the current gain characteristics as a function of  $J_c$ . The current gain does not depend on the emitter-base spacing. In addition, the current gain for the HBT with a 0.25- $\mu\text{m}$ -emitter is comparable to that for the HBT with a 50- $\mu\text{m}$ -emitter. On the basis of these results, we conclude that this ledge structure sufficiently suppresses the surface recombination current.

Figure 5 shows the current gain ( $h_{21}$ ) and Mason's unilateral gain ( $UG$ ) as a function of frequency. The  $f_t$  and  $f_{\text{max}}$  were obtained by extrapolation of  $h_{21}$  and  $UG$  with -20 dB/decade slope line. Figure 6 summarizes the  $f_t$ ,  $f_{\text{max}}$ , and total collector capacitance,  $C_{\text{TC}}$ , as a function of  $J_c$ . The HBT exhibits an  $f_t$  of 442 GHz and  $f_{\text{max}}$  of 214 GHz at a  $J_c$  of  $12 \text{ mA}/\mu\text{m}^2$ . The  $C_{\text{TC}}$  is 11 fF. The  $f_{\text{max}}$  is relatively low, which is due to the large base resistance. The  $f_{\text{max}}$  could be improved by using a pseudomorphic base [3].

### 4. Conclusions

We have demonstrated 0.25- $\mu\text{m}$ -emitter InP HBTs with a passivation ledge structure. The HBTs exhibit a reasonably high current gain of over 60 and an  $f_t$  of 442 GHz. These results indicate that this technology is promising for making high-speed 0.25- $\mu\text{m}$ -emitter InP HBTs with a reasonably high current gain.

### Acknowledgements

Part of this work was supported by SCOPE from the Ministry of Internal Affairs and Communications.

### References

- [1] W. Snodgrass, W. Hafez, N. Harft, and M. Feng, *Tech. Dig. Proc. Int. Electron Device Meeting (IEDM)*, 2006, pp. 11
- [2] N. Kashio, K. Kurishima, Y. K. Fuka, M. Ida, and S. Yamahata, *Proc. 2009 IEICE general conference*, 2009, C-10-10.
- [3] M. Ida, K. Kurishima, and N. Watanabe, *IEEE Electron Device Lett.*, vol. 23, no. 12, pp. 694, 2002.

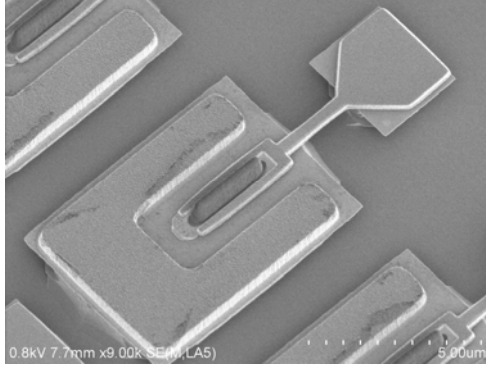


Fig. 1. SEM image of a fabricated HBT with an emitter size of 0.25  $\mu\text{m}$  x 3  $\mu\text{m}$ .

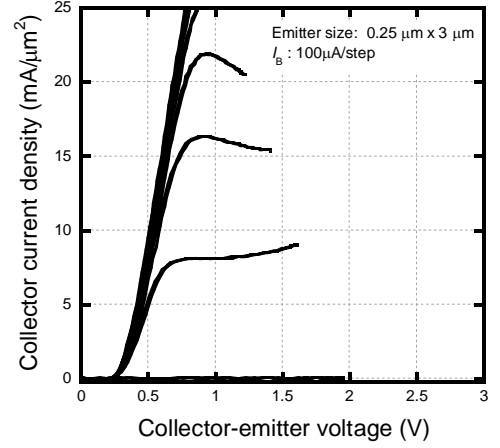


Fig. 2. Common-emitter collector I-V characteristics for the HBT with an emitter size of 0.25  $\mu\text{m}$  x 3  $\mu\text{m}$ .

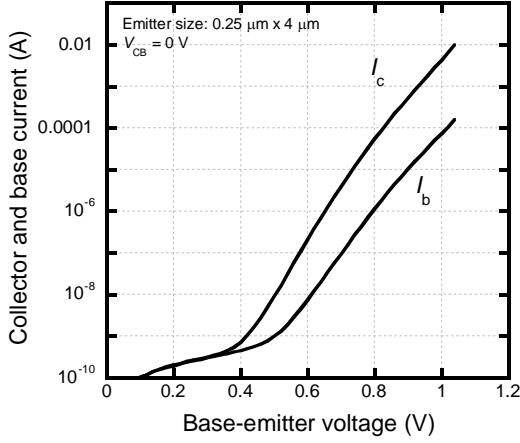


Fig. 3. Gummel plot of the HBT with an emitter size of 0.25  $\mu\text{m}$  x 4  $\mu\text{m}$ . The collector-base voltage,  $V_{CB}$ , is 0 V.

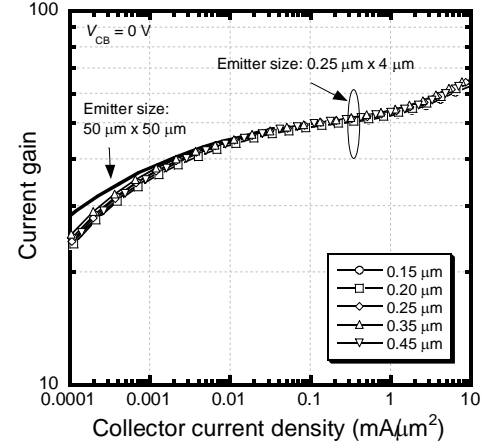


Fig. 4. Current gain characteristics for HBTs with various emitter-base spacing.

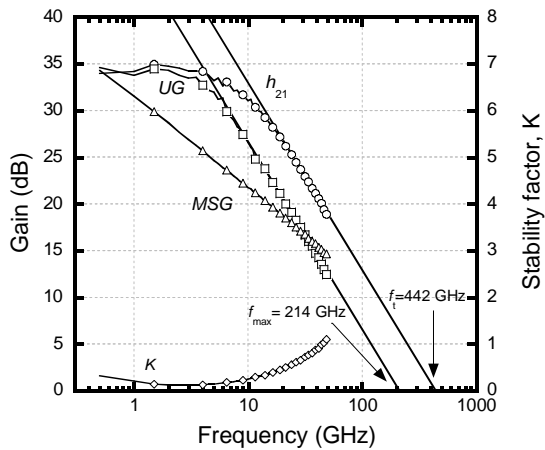


Fig. 5. Current gain ( $h_{21}$ ), Mason's unilateral gain ( $UG$ ), maximum stable gain ( $MSG$ ), and stability factor,  $K$ , as a function of frequency.

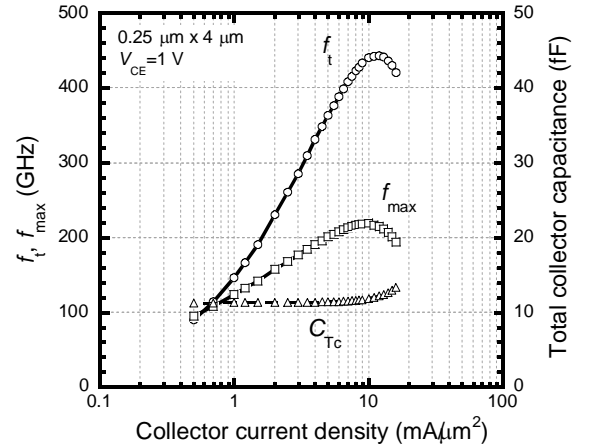


Fig. 6.  $f_t$ ,  $f_{max}$ , and total collector capacitance,  $C_{Tc}$ , as a function of collector current density.